available at www.sciencedirect.com

ScienceDirect

www.elsevier.com/locate/brainres

BRAIN RESEARCH

Research Report

Multiple neurogenic and neurorescue effects of human mesenchymal stem cell after transplantation in an experimental model of Parkinson's disease

Lidia Cova[a,*,1], *Marie-Therese Armentero*[b,1], *Eleonora Zennaro*[a], *Cinzia Calzarossa*[a], *Patrizia Bossolasco*[c], *Giuseppe Busca*[d], *Giorgio Lambertenghi Deliliers*[e], *Elio Polli*[c], *Giuseppe Nappi*[b,f], *Vincenzo Silani*[a,2], *Fabio Blandini*[b,2]

[a]*Department of Neurology and Laboratory of Neuroscience, Centro "Dino Ferrari", Università degli Studi di Milano-IRCCS Istituto Auxologico Italiano, 20149 Milan, Italy*
[b]*Laboratory of Functional Neurochemistry, Interdepartmental Research Center for Parkinson's Disease, IRCCS Neurological Institute "C. Mondino", 27100 Pavia, Italy*
[c]*Fondazione Matarelli, Università degli Studi di Milano, Department of Pharmacology, Chemotherapy and Medical Toxicology, Università degli Studi di Milano, 20129 Milan, Italy*
[d]*Medical Cardiovascular Institute, Maggiore Hospital Policlinico Mangiagalli e Regina Elena - IRCCS, 20122 Milan, Italy*
[e]*U.O. Ematologia 1 - CTMO, Fondazione Ospedale Maggiore Policlinico and Università degli Studi di Milano, Italy*
[f]*Chair of Neurology, University of Rome "La Sapienza", 00185 Rome, Italy*

ARTICLE INFO

Article history:
Accepted 18 November 2009
Available online 26 November 2009

Keywords:
Striatum
6-hydroxydopamine
Cytokine
Subventricular zone
Neurogenesis

ABSTRACT

Stimulation of endogenous repair in neurodegenerative diseases, such as Parkinson's disease (PD), appears to be a novel and promising therapeutic application of stem cells (SCs). In fact SCs could propel local microenvironmental signals to sustain active endeavors for damaged neurons substitution, normally failing in non-supportive pathological surroundings. In this study, we demonstrated that two different doses of naïve human adult mesenchymal stem cells (hMSCs), implanted in the striatum of rats lesioned with 6-hydroxydopamine (6-OHDA), positively survived 23 days after transplantation. Their fate was directly influenced by the surrounding host environment while grafted hMSCs, dose dependently, regionally sustained the survival of striatal/nigral dopaminergic terminals and enhanced neurogenesis in the Subventricular Zone (SVZ). The number of proliferative cells (Ki67/Proliferating Cell Nuclear Antigen +) as well as neuroblasts migration significantly augmented in the lesioned striatum of transplanted animals compared to controls. No SVZ astrogenesis was detected in all experimental conditions, irrespectively of graft presence. Activation of endogenous stem cell compartments and rescue of dopaminergic neurons, supported by the persistent release of specific cytokine by MSCs *in vivo*, appeared in

* *Corresponding author*. Department of Neurology and Laboratory of Neuroscience, Centro "Dino Ferrari", Università degli Studi di Milano-IRCCS Istituto Auxologico Italiano, via Zucchi 18, 20095 Cusano Milanino, Milan, Italy. Fax: +39 02 619113033.
E-mail address: l.cova@auxologico.it (L. Cova).

Abbreviations: 6-OHDA, 6-hydroxydopamine; CNS, central nervous system; Dcx, double cortin; GFAP, glial fibrillary acidic protein; NSC, neural stem cells; PD, Parkinson's disease; PCNA, proliferating cell nuclear antigen; SVZ, subventricular zone; TH, tyrosine hydroxylase

[1] These authors contributed equally to this work.
[2] Joint senior authors.

doi:10.1016/j.brainres.2009.11.041

principle able to contrast the neurodegenerative processes induced by the 6-OHDA lesion. Our results suggest that reciprocal influences between grafted cells and endogenous neural precursors could be important for the observed neurorescue effect on several brain regions. Altogether, our data provide remarkable cues regarding the potential of hMSCs in promoting endogenous reparative mechanisms that may prove applicable and beneficial for PD treatment.

1. Introduction

The pathological hallmark of Parkinson's disease (PD) is the progressive dopaminergic depletion, caused by the selective death of neuronal subpopulations, projecting to the corpus striatum from the *Substantia Nigra pars compacta* (*SNpc*). To date, the pharmacological replacement of the deficient neurotransmitter dopamine (DA) with its direct precursor, L-3,4-dihydroxyphenylalanine (L-DOPA), remains the gold standard therapy. However, long-term treatment with L-DOPA is associated with considerable side effects and does not modify the progression of the disease, which evolves synchronous with the continuous and progressive degeneration of residual dopaminergic neurons (Dass et al., 2006). DA is also implicated in developmental and adult neurogenesis (Borta and Hoglinger, 2007) which appears significantly impaired in PD patients (Hoglinger et al., 2004). Activation of progenitor cells residing in the subventricular zone (SVZ), one of the adult neurogenic region, has been extensively described (Nam et al., 2007; Quinones-Hinojosa et al., 2006), and shown to increase proliferation and differentiation in response to neuronal loss (Sundholm-Peters et al., 2005). Moreover, striatum is connected to both SVZ and *SNpc* by dopaminergic afferents which are relentlessly impaired by age and disease (Freundlieb et al., 2006; Hoglinger et al., 2004). Neural stem cells (NSCs) reside in highly vascularized (neurovascular/neurogenic) niches where the complex dynamic interplays between neurons and stromal/endothelial cells are similarly mediated via neurotrophine activated pathways (Martino and Pluchino, 2006). Moreover, modulation of DA receptor may trigger neuronal differentiation of adult SVZ cells both *in vitro* (Coronas et al., 2004) and *in vivo* (Van Kampen and Eckman, 2006; Van Kampen et al., 2004). Therefore, although the regenerative capacity of the pathological central nervous system (CNS) remains controversial (Hermann and Storch, 2008), enhancement of endogenous repair may represent an attractive alternative strategy for the therapeutic treatment of PD (Okano et al., 2007).

Stem cell (SC)-based therapies, through the production of diffusible trophic factors, may effectively support activation of neurogenesis, as well as migration, maturation and integration of newly generated neurons in a functional network (Okano et al., 2007). To date, bone-marrow-derived cells, comprising both human hematopoietic and mesenchymal stem cells (hMSCs), represent a major source of exogenous adult progenitor cells capable to regenerate and repair tissues (Han et al., 2006). Several reports have demonstrated that MSCs have the potential to directly differentiate into multiple cellular types, such as myogenic progenitors, neural cells and hepatocytes (Giordano et al., 2007), and, more importantly, to produce factors promoting the expansion/differentiation of hematopoietic stem cells (Caplan and Dennis, 2006). Many data also suggest that the hMSC-mediated restoration of injured tissues may depend upon their capacity to release a broad spectrum of cytokines/growth factors inhibiting apoptosis, promoting angiogenesis and stimulating the host cells to regenerate the damaged tissues (Dezawa et al., 2005). Another interesting and intriguing feature of hMSCs relies on their capability to avoid immune system recognition and to establish immune-response inhibition (Rasmusson, 2006). Therefore, several of the complex interconnected biological pathways triggered by MSC implantation correspond to proposed multiple pathogenic targets in PD (Hodaie et al., 2007). Finally, hMSCs may be allogeneically harvested and expanded making them ideal candidates for clinical use.

The aim of the present study was to investigate the neurogenic (and neurorescue) potential of hMSCs, after intra-striatal transplantation, in the experimental 6-hydroxydopamine (6-OHDA) rodent model of PD, as paradigm of future cell therapy applications. We were particularly interested in the two regions physically connected to striatum by dopaminergic afferents: SVZ and *SNpc*.

2. Results

In order to assess the hMSCs therapeutic potential in injury and/or disease, we tested their capability to activate SVZ neurogenesis and to rescue dopaminergic neuron degeneration caused by intra-striatal infusion of 6-OHDA, an animal model closely resembling the progressive human pathology (Blandini et al., 2008; Deumens et al., 2002).

Two different concentrations (low, 32,000 or high amount, 180,000) of Hoechst-labeled hMSCs, or vehicle (PBS), were grafted into the ipsilateral striatum of 6-OHDA and SHAM animals, 5 days after the toxic insult that triggered nigrostriatal neurodegeneration (Fig. 1). To avoid possible reject of the xenotransplant and to mimic standard clinical procedures, all animals received a daily injection of cyclosporine A, a treatment that *per se* had no influence on the toxin-induced degenerative process, inflammatory response or transplanted human cells (Supplemental Fig. 1).

2.1. *Neurogenic effect of transplanted hMSCs*

We assessed the effect of hMSC transplantation on the host neurogenic activity through the combined detection of anti-rat Ki67 (expressed in all cell cycle phases, except G0), Proliferating Cell Nuclear Antigen (PCNA; present in G1/S phase), Nestin (marker of neural progenitor cells) and double cortin (Dcx; marker of migrating neuroblasts) (Figs. 2–5).

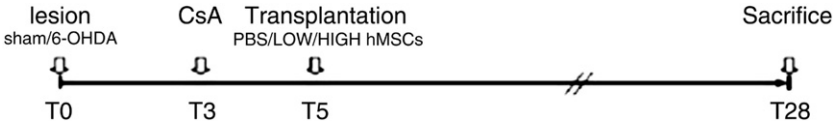

Fig. 1 – Experimental procedures and groups. Schematic representation of the *in vivo* experimental procedures. The time course (T) of the experiments is indicated in days; animals received an intra striatal injection of 6-OHDA or vehicle (SHAM animals) (T0), and were transplanted 5 days (T5) later with hMSCs or PBS. Rats were sacrificed 23 days later (T28 from lesion). Daily intraperitoneal injections of cyclosporine A (CsA, 10 mg/kg) were started 3 days (T3) after the first surgical procedure (T0).

2.1.1. hMSCs efficiently support endogenous proliferation in the SVZ

We initially characterized proliferative events in the stem compartment of SVZ through a densitometric quantification of the quiescent population characterized by a prolonged cell cycle (Ki67+ cells, green) vs. the mitotically active cells (PCNA+ cells, red) in lesioned, transplanted animals. Nuclear Ki67- and PCNA-immunopositive cells (respectively green and red) were

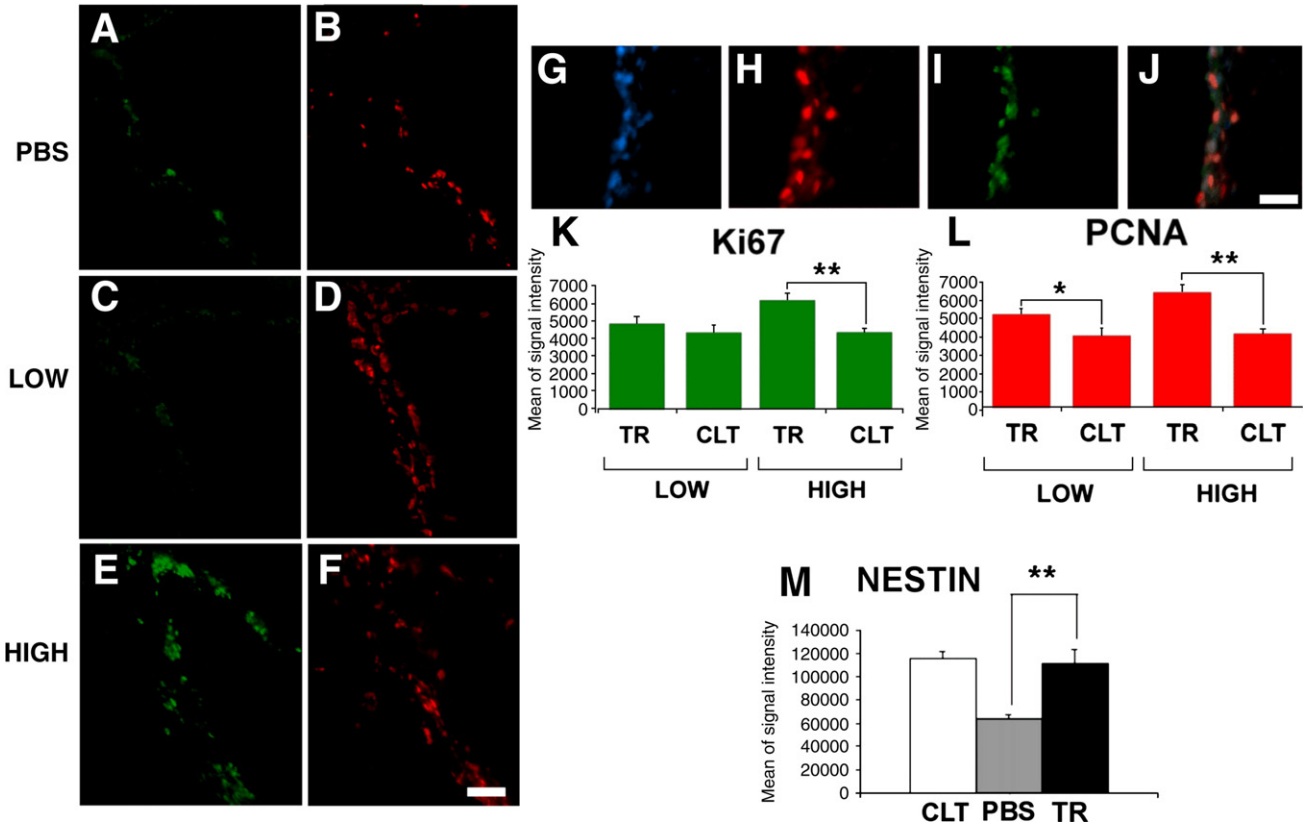

Fig. 2 – Densitometric analysis of proliferation and neural progenitor cells. The whole ependymal layer was captured at low magnification and quantified in order to verify graft influence on host biology. (A–F) Representative fields of lesioned SVZ implanted with PBS (A,B), Low (C,D) and High (E,F) dose of hMSCs: thickening of stem cells residing region is clearly distinguishable. Specific nuclear localization was demonstrated by DAPI (blue, G), PCNA (red, H), Ki67 (green, I) and merge (J) pictures. (K,L) Graphs demonstrating the intensity signals for the Ki67+ (red) and PCNA+ cells (green) throughout the entire striatum after hMSC transplantation. Results (mean ± SEM) are expressed as the mean of signal intensity for PCNA or Ki67 positive regions in the injected striatum respect to the intact contralateral hemisphere. CLT = 6-OHDA contralateral brain side; TR = 6-OHDA transplanted brain side. *$p < 0.05$ vs. mean of signal intensity for PCNA immunoreactivity in the SVZ of Low hMSC implanted animals (two sided, paired Student's *t*-test). **$p < 0.01$ vs. percentage mean of signal intensity for PCNA or Ki67 immunolabeling in the SVZ of high hMSC implanted animals (two sided, paired Student's *t*-test). (M) Quantitative comparison of Nestin+ cells in the SVZ in 6-OHDA lesioned animals demonstrated active differentiation towards progenitor cells after hMSC graft. PBS = 6-OHDA saline injected brain side; CLT = 6-OHDA Contralateral brain side; TR = 6-OHDA Transplanted brain side. Results (mean ± SEM) **$p < 0.05$ percentage mean of signal intensity in the SVZ of PBS implanted animals vs. both CLT and TR animals (two sided, paired Student's *t*-test). In lesioned PBS implanted animals immunoreactivity was slightly increased in the ipsilateral hemisphere with respect to the non-lesioned hemisphere, possibly reflecting a proliferative response to the mechanical injury due experimental procedures (not shown). A total number of 18 coronal sections for rat and 4 animals were used for every experimental condition. (A–F) Ki67+ cells (green) and PCNA+ cells (red); scale bar: 100 μm. (G–J) scale bar: 50 μm.

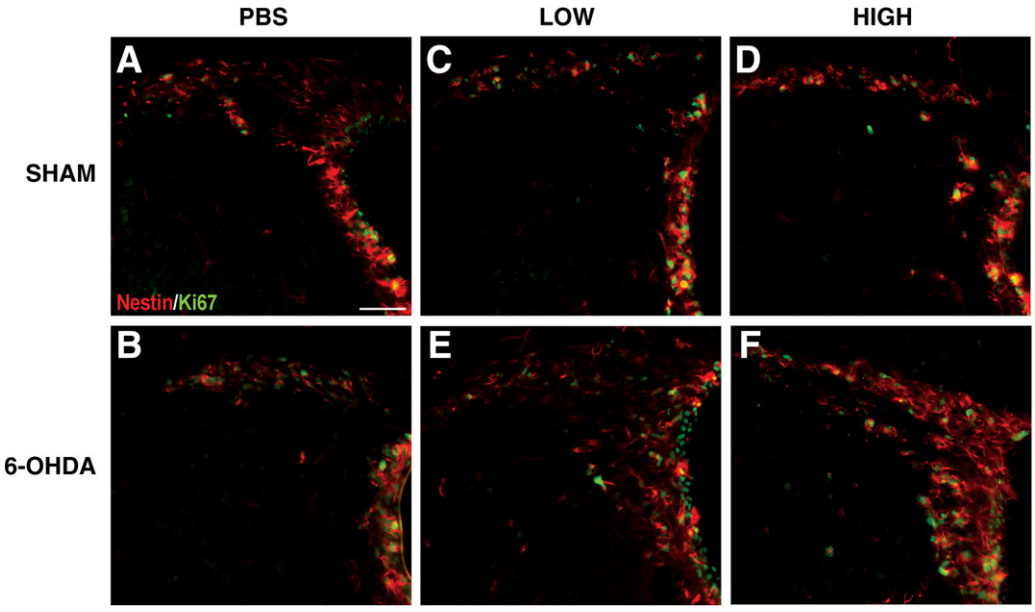

Fig. 3 – Enhanced proliferation and maturation of neural progenitor after transplantation in lesioned rats. SHAM (PBS, A; hMSC Low amount, C; hMSC High amount, D) and 6-OHDA-lesioned animals (PBS, B; hMSC Low amount, E; hMSC High amount, F). Increased Ki67 labeling in ependymal layers appears dose dependently related to hMSC implantation in lesioned brains (compare figure C vs. E and D vs. F). Similarly, host Nestin+ progenitor activation was observed with a maximum effect at high hMSC dose in the intoxicated brains (compare C, D to E, F). Scale bar: 50 μm (G,H).

unevenly distributed along the SVZ (Figs. 2A–F), but their density was influenced by the graft presence and dose (compare Figs. 2A,B vs. C,D and E,F). PCNA and Ki67 nuclear localization was confirmed by DAPI (blue) staining in the same field, as shown in Figs. 2G–J).

Our densitometric results indicate that hMSC presence induced a significant increase (signal intensity) of the area containing quiescent and proliferating cells in the ipsilateral SVZ (Fig. 2K, Ki67 green and L, PCNA, red). Interestingly, a significant increase of Ki67 labeling was detected only in animals receiving the highest number of human cells ($p<0.01$ vs. the contralateral hemisphere, Fig. 2K), while levels of nuclear PCNA expression were significantly enhanced in lesioned animals transplanted with low ($p<0.05$ vs. the contralateral hemisphere) and high amount of hMSCs ($p<0.01$ vs. the contralateral hemisphere) (Fig. 2L). Cell proliferation in 6-OHDA lesioned-vehicle implanted animals was comparable to the non-lesioned hemisphere (data not shown).

Altogether, our data demonstrated that graft presence directly enhanced proliferation in the ependymal layer in a dose dependent manner.

2.1.2. *Neural progenitor development is sustained by grafted MSCs*

Since any therapeutic application requires increased differentiation towards stem/progenitor cells and then migrating neuroblasts, we also performed a densitometric quantification of Nestin+ cells (specifically expressed by 79% of all neuroblasts and neural progenitors) along the whole SVZ of 6-OHDA-lesioned animals (as detailed in Experimental procedures). Intrastriatal injection of the neurotoxin reduced the number of neural progenitor cells in the lesioned hemisphere compared to the contralateral side ($p<0.05$) (Fig. 2M). Transplantation of hMSCs significantly enhanced the amount of Nestin+ cells that returned to physiological levels, thus suggesting that neural progenitor cell appearance is inhibited after 6-OHDA lesion, but supported by hMSC graft.

Consequently, we combined Nestin and Ki67 detection (Figs. 3A–F) to study the correct neural stem cell localization as well as SVZ cytoarchitecture. In SHAM animals transplanted with hMSCs or vehicle, Nestin labeling for neural progenitors stained cellular subsets with filamentous shape, dispersed along SVZ towards striatum and rarely co-localized with Ki67+ proliferating cells (see Figs. 3A, C, D, Nestin+ cells, red and Ki67+ cells, green). Round proliferating Ki67+ cells were physiologically found in the wall of the lateral ventricle in both SHAM/lesioned animals (Figs. 3A, C, D). The number of Ki67+ cells was not visibly modified by intra-striatal injection of 6-OHDA (compare Figs. 3A and B), while it increased after grafting of hMSCs (compare SHAM and 6-OHDA treated animals, Figs. 3C, D to E, F, Ki67+ cells, green, concordantly to densitometric data). Conversely, an important enhancement of labeling intensity and SVZ thickening was detected for both markers following transplantation of hMSCs in lesioned animals (compare Figs. 3C, D and E, F). Interestingly, the number of Nestin+ progenitor cells in the ipsilateral SVZ was particularly increased in lesioned animals that received a large amount of hMSCs (Fig. 3F, Nestin+ cells, red).

We then estimated the dispersion of newborn neuronal cells by means of double Nestin/Dcx immunolabeling (Fig. 4, respectively red and green). The zone of Nestin/Dcx co-localization was wider in transplanted 6-OHDA-lesioned rats in comparison to SHAM hMSC injected animals (compare Figs. 4E, F to B, C). Gradual phenotypic cell maturation and

neuralization, was accompanied by a shift from the subependymal to inner striatal layers, as proven by the presence of Dcx immunoreactive neuroblasts in this region (Figs. 4E, F, Dcx+ cells, green). Transplantation of hMSCs in lesioned animals visibly increased Dcx expression and induced the migration of ramified neuroblasts towards lesioned striatum (Figs. 4E′, F′).

2.1.3. *MSC presence selectively enhanced neurogenesis*

Double fluorescent labeling for both Ki67 and Dcx allowed the clear distinction between proliferative cells (Ki67+ cells) mainly localized in the lateral ventricle and neuroblasts dispersed in inner striata (Fig. 5, respectively red and Dcx, green cells).

Presence of the lesion influenced SVZ proliferation and clearly reduced the neuroblast number when compared to SHAM/PBS injected animals (compare Figs. 5A, D). Neuroblast dispersion into striatum directly related to grafted cell dose (Figs. 5B, C, E, F) and was particularly enhanced in 6-OHDA animals (Figs. 5E, F). In SHAM animals even after cell graft, proliferation and neural marker expressions were physiologically low 28 days and few Dcx stained cellular subsets are localized into striatum (compare Figs. 5A–C to D–F).

Increased striatal neurogenesis also requires minimal acquisition of astroglial fate; therefore, the presence of astrocytes in the SVZ, immediately adjacent to the lateral ventricle, was qualitatively assessed by the Glial Fibrillary Acidic Protein (GFAP) staining in both transplanted and contralateral side of 6-OHDA brains (Figs. 5G–L, GFAP+ cells, green). The number of GFAP+ cells and labeling intensity were akin between the different conditions in transplanted animals (compare PBS/Low/High in the contralateral Figs. 5G–I vs. transplanted side, Figs. 4J–L), although transplantation of the largest amount of hMSCs induced astrocyte hypertrophism, in both hemispheres (Figs. 5I, L).

In summary, our data showed that SVZ, dose dependently, boosted persisting proliferation and neuronal maturation 23 days after hMSC transplantation, while no astrogenesis processes were detectable, thus enlightening the specific graft-dependent action on striatal neurogenesis.

2.2. *Reciprocal interactions influence both host tissue and grafted hMSC characteristics*

Fluorescent examination of transplanted striata indicated that grafted hMSCs readily survived throughout the lesioned striatum. Interestingly, the amount of human cells detectable after 4 weeks was proportional to the initial number of hMSCs at the time of transplantation (Supplemental Fig. 2A,B). In fact,

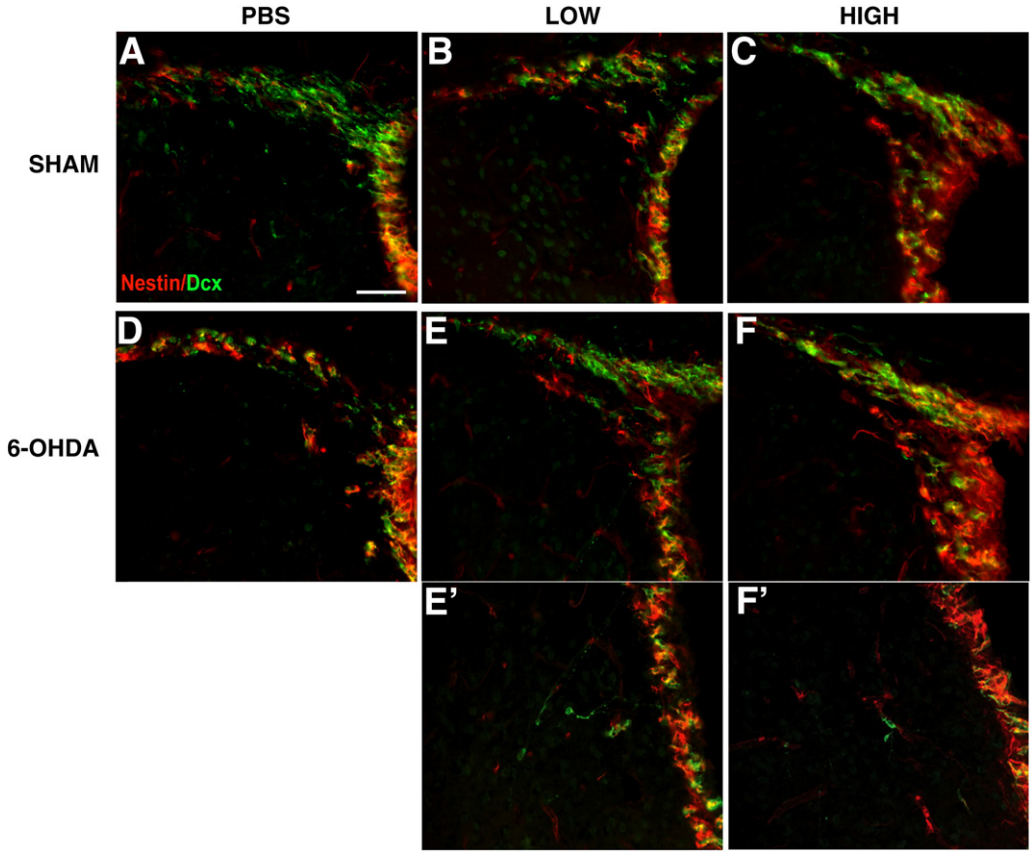

Fig. 4 – Grafted hMSCs positively influence neural progenitor and neuroblast numbers in the SVZ. (A–F) Proliferative and neuronal progenitor marker stainings are shown for SHAM (PBS, A; hMSC Low amount, B; hMSC High amount injected, C) and lesioned animals (PBS, D; hMSC Low amount, E; hMSC High amount injected, F). hMSC transplantation slightly enhanced differentiation of neural progenitors in the ependymal layers (Nestin+ cells, red, A–F) towards migrating (Dcx+ cells, green) neuroblasts even in SHAM brain (B, C). (E′,F′) Ramified neuroblasts are dispersed in the inner striatal layers showing a spatial integration only in 6-OHDA-Low/High animals. Scale bar: 50 μm.

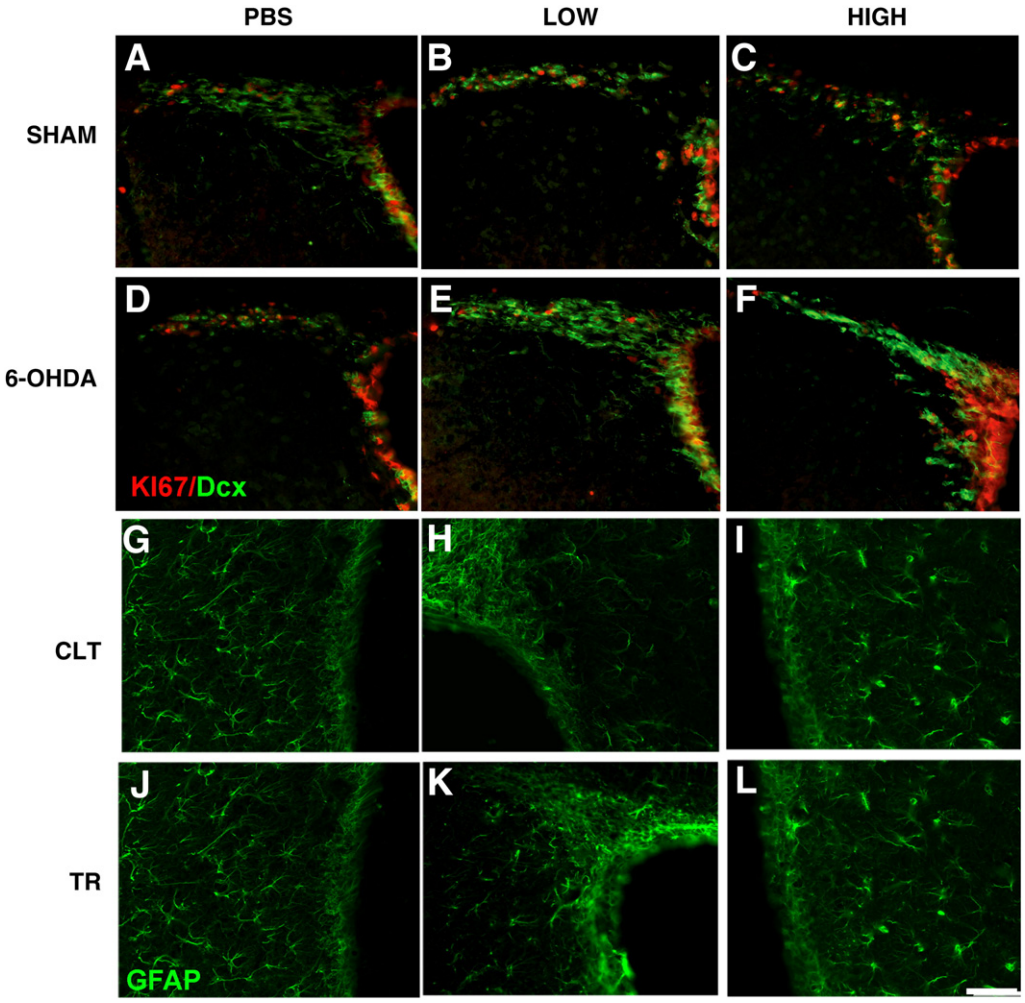

Fig. 5 – Neurogenesis rate is selectively enhanced by grafted cells. The paraphysiological situation in SHAM animals for progenitor and neuroblast markers is shown for SHAM (PBS, A; hMSC Low amount, B; hMSC High amount, C) and lesioned animals (PBS, D; hMSC Low amount, E; hMSC High amount, F). hMSC transplantation slightly enhanced maturation of ependymal proliferative cells towards migrating (Dcx+) neuroblasts even in the lesioned striata of SHAM brains (B, C and E, F). Neuroblast ratio was directly and independently influenced by 6-OHDA injection, hMSC transplantation, as well as by the combination of striatal degenerated environment and implanted human cells (compare B, C vs. E, F). (G–L) In 6-OHDA treated rats, GFAP labeling intensity and region thickening appeared comparable in all experimental conditions, irrespectively of graft presence, although a slight signal increase can be observed in injected hemispheres, probably due to the mechanical procedures (compare G–I to J–L). Notably, high cell dose specifically induced a negligible glial hypertrophy in both hemispheres (compare H,I to K,L). LV = Lateral Ventricle. CLT = 6-OHDA Contralateral brain side; TR = 6-OHDA Transplanted brain side. Scale bar: 50 μm.

a relative count of surviving Hoechst-positive hMSCs detected in striatal sections (as described in Experimental procedures) indicated that survival of transplanted cells was proportionally maintained in favor of the highest number of hMSCs. Bar extending above the dotted line demonstrates that, after transplantation, the ration was still maintained in favor of the high group, indicating that the amount of cells surviving correlates with the initial amount at the time of transplantation (Supplemental Fig. 2C). In addition, transplanted cells did not migrate, remaining all gathered around the injection site (Supplemental Fig. 2A,B) and showed no appreciable apoptotic (TUNEL+) or proliferative phenomena (Ki67+/total human cell number as described in Experimental procedures) (not shown).

The intrastriatal injection of 6-OHDA induced an important loss of dopaminergic terminals in the striatum as detected 28 days after lesion (Supplemental Fig. 2D). Transplantation of Hoechst 33528-labeled hMSCs in the ipsilateral striatum, 5 days after the toxic insult, resulted in a reduced drug-induced loss of dopaminergic terminals throughout the striatum. Interestingly, sparing of TH terminals was particularly marked in the rostral part of the nucleus corresponding to the striatal region nearest to graft site ($p < 0.01$ 6-OHDA-Low/High grafted groups vs. 6-OHDA-vehicle group) and related to the amount of human cells transplanted (Supplemental Fig. 2D). In SHAM animals, hMSC transplantation *per se* did not modify the density of striatal DA terminals (data not shown). Grafting of both amounts of hMSCs also significantly increased the

number of spared dopaminergic cell bodies in the ipsilateral *SNpc* (Supplemental Table 1) compared to lesioned animals that received vehicle ($p<0.05$ 6-OHDA-Low/High grafted groups vs. 6-OHDA-vehicle group).

Unambiguous identification of grafted cells was confirmed by specific anti human NuMA staining (Fig. 6A) and morphological analysis of the striatum showed that transplantation of high cell number *per se* did not damage the surrounding tissue. hMSCs evidently adapted to their surroundings since the typical spindle, large flat morphology, and ubiquitous Nestin expression, were normally observed *in vitro* (Fig. 6B), but resulted drastically reduced after grafting. Indeed, 23 days after transplantation of the lowest amount of hMSCs, the cells assumed a more oval shape, reduced their cytoplasm and only few expressed Nestin antigens (Fig. 6C, Nestin+ cells, green). In addition, few sparse round hMSCs also co-expressed GFAP (see representative image in Fig. 6C, GFAP+ cells, red), a neural antigen never detected *in vitro*. Interestingly, complete loss of Nestin expression in conjunction with the appearance of GFAP+ hMSCs was observed only when a higher amount of cells were transplanted (Fig. 6D). Emergence of neuronal progenitor markers was never observed in grafted hMSCs, indicating that they did not undergo any neuronal maturation after transplantation (not shown). Therefore, the positive effects exerted by MSCs on the striatum did not rely on the orthotopic dopaminergic neurogenesis nor on neuronal trans-differentiation of grafted cells.

Immunohistochemical evaluation of striatal sections from SHAM-hMSC transplanted animals showed that the human cells similarly survived, without detectable suffering features, and lost expression of Nestin cytoplasmic networks, but never acquired human specific GFAP immunopositivity (Fig. 6E).

2.3. *Cultured hMSCs produce a broad spectrum of (neuro) trophic and angiogenic factors*

Since hMSC effect on distal SVZ regions may depend upon cytokine/growth factor release, we performed a qualitative evaluation of 120 different chemokines and cytokines in naïve, cultured hMSCs (see details in Experimental procedures). Significantly, 84 trophic factors were commonly

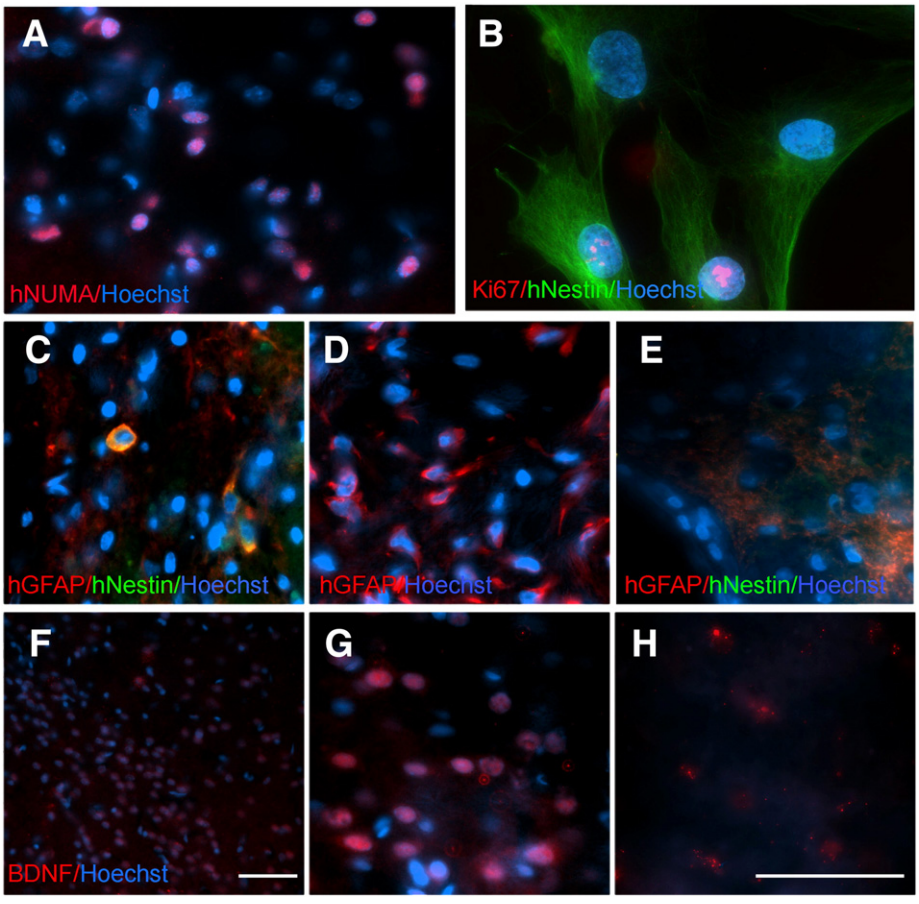

Fig. 6 – Reciprocal influences between implanted striata and grafted cells. (A) The human origin of grafted cells was confirmed by specific anti human NuMa antigen identification. (B–E) Although naïve hMSCs in cultures present a complex human specific Nestin+ cytoplasmic network (B), after graft, we observed sparse hMSCs positively stained for human-specific GFAP and Nestin in 6-OHDA-Low animals (C), while most implanted hMSCs in 6-OHDA-High animals demonstrated only acquisition of human specific GFAP staining (D). Cytoplasm size was severely reduced after implantation (compare B to C, D). (E) No human specific Nestin or GFAP labeling was present in SHAM grafted animals. (F, G) BDNF expression co-localized only with hMSCs while no signal was detected in lesioned PBS implanted animals (H). Scale bars: 50 μm (F) and 10 μm (A–E and G, H).

Table 1 – Detection of chemokine, cytokine synthesis and neuro/angiogenic factors in hMSCs.

A

Cytokines	CM	LYS	Cytokines	CM	LYS	Cytokines	CM	LYS	Cytokines	CM	LYS	Cytokines	CM	LYS	Cytokines	CM	LYS
Acrp30	-	+	CCL20	-	+	FGF-2	+	+	IFN-γ	-	+	IL-8	+	+	sTNF RI	+	+
AgRP	-	+	CCL23	+	+	FGF-4	-	-	IL-1β	+	+	I-TAC	+	+	sTNF RII	+	+
Ang-2	-	+	CCL24	+	+	FGF-7	+	+	IL-6	+	+	MCP-2	-	+	TECK	-	-
AR	-	+	CCL26	+	+	FGF-9	-	+	IL-6 R	+	+	MCP-4	-	+	TGF-β3	-	+
AXL	-	+	CCL28	-	+	GCSF	-	+	IGFBP-2	+	+	MIF	-	+	THPO	-	-
BCL	-	-	CCL5	+	+	FLT-3 L	+	+	IGF-I SR	-	+	MIP-1β	-	+	TIMP-1	+	+
BDNF	+	+	CCL5	+	+	GDNF	-	+	IL-1 R4	-	+	MIP-1α	-	+	TIMP-2	+	+
BMP-4	+	+	CTACK	-	+	GITR	+	+	IL-12 p70	-	+	NT-3	+	+	TNF-α	-	+
bNGF	-	+	CTNF	+	+	GITR L	-	+	IL-15	-	+	NT-4	-	-	TNF-β	-	+
BTC	-	+	CX3CL1	+	+	GRO	+	+	LIGHT	+	+	OPG	+	+	TRAIL R3	-	+
CCL1	-	+	CXCL7	+	+	GRO-α	+	+	IL-1α	+	+	OSM	-	-	TRAIL R4	-	+
CCL16	+	+	EGF	+	+	HGF	+	+	IL-2 Rα	+	+	SCF	+	+	UPAR	+	+
CCL17	+	+	EGF-R	-	+	IL-1 ra	+	+	IL-3	+	+	SDF-1	-	+	VEGF	+	+
CCL2	+	+	FAS	-	+	ICAM-1	+	+	IL-4	+	+	sgp130	+	+	VEGF-D	+	+

B) Multiplex analysis for angiogenic factors in CMs

Samples	ANG2 pg/ml	FGF-2 pg/ml	HB-EGF pg/ml	HGF pg/ml	KGF pg/ml	PDGF-BB pg/ml	THPO pg/ml	TIMP1 pg/ml	VEGF pg/ml
BM (no MSCs)	0	0	6.00±3.11	10.70±1.56	0	0	0	54.8±24.61	0
CM from Confluent MSC	185.05±95.95	40.45±17.61	140.85±52.40	613.2±214.54	636.95±190.42	39.25±13.08	178.2±44.83	>2500	>2500
CM from Proliferative MSC	83.15±16.48	15.10±1.41	75.10±0.99	100.9±42.57	145.75±93.55	11.55±2.33	91.45±13.93	>2500	>2500

CM: conditioned medium LYS: cell lysates.

-: decreased expression in CM compared to BM levels in the absence of MSCs (metabolic uptake, CM)/absent (LYS).

+: increased expression compared to BM levels in the absence of MSCs (metabolic secretion, CM)/present (LYS).

Abbreviations: AgRP/Adiponectin: Agouti-related Protein; AR: Amphiregulin; Ang-2: Angiopoietin-2; AXL: AXL receptor tyrosine kinase; BDNF: Brain-Derived Neurotrophic Factor; bFGF: basic Fibroblast Growth Factor; BMP 4: Bone morphogenetic protein 4; b-NGF: brain Nerve Growth Factor; BTC: Betacellulin; CCL1/I-309: Th2-related C-C chemokine I-309; CCL16/HCC-4: also named NCC-4, liver-expressed chemokine (LEC), and lymphocyte and monocyte chemoattractant (LMC), CCL17/TARC: TARC Thymus- and activation-regulated chemokine; CCL18/PARC: pulmonary and activation-regulated chemokine; CCL2/MCP-1: monocyte chemotactic protein-1; CCL20/ MIP-3β: Macrophage Inflammatory Protein β; CCL23/CK β 8-1: chemokine (C-C motif) ligand 23; Creatine Kinase BB; CCL24: Eotaxin-2; CCL26:Eotaxin-3; CCL-28/MEC mucosae-associated epithelial chemokine; CL5/RANTES: regulated upon activation normal T cell expressed and secreted; CNTF: Ciliary Neurotrophic Factor; CTACK: Cuteaneous T-Cell Attracting Chemokine; CX3CL1: Fractalkine; CXCL7/NAP-2: neutrophil activating peptide-2; EGF: Epidermal Growth Factor; EGF-R: Epidermal Growth Factor Receptor; FGF-2/4/7/9: Fibroblast Growth Factors 4/7/9; FLT-3 Ligand: Fms-related tyrosine kinase 3 ligand; *GCSF:* granulocyte-colony stimulating factor; *GDNF*: Glial cell derived neurotrophic factor; *GITR:* glucocorticoid-induced tumor-necrosis-factor-receptor; *GITR-Ligand*: glucocorticoid-induced tumor-necrosis-factor-receptor Ligand; GRO: monocyte attracting chemokines like growth related oncogene; GROα: monocyte attracting chemokines like growth related oncogene; HGF: Hepatocyte Growth Factor; ICAM-1: Intercellular Adhesion Molecule-1; IFN-γ: *Interferon-Gamma*; IGFBP-2: Insulin-like growth factor binding protein 2; IL-1 β: *Interleukin-1 beta*; IL-1 R4/ST2: *Interleukin* 1 receptor 4, also known as ST2; IL-1 ra: Inhibitor IL-1 receptor antagonist; IL-12 p70: bioactive IL-12 molecule; IL-15: Interleukin-15; IL-1α: Interleukin-1 α; IL-2 R α: IL-2 receptor chain α; IL-3/4/6: Interleukin-3/4/6; IL-6 R: Interleukin-6 receptor; IL-8: Interleukin-8; I-TAC: Interferon-inducible T Cell Alpha Chemoattractant; LIGHT: tumor necrosis factor (TNF) superfamily ligand; MCP-2: Monocyte chemotactic protein 2; MCP-2: Monocyte chemotactic protein 4; *MIF:* Macrophage migration inhibitory factor; MIP-1α/β: Monocyte chemoattractant proteins-1α/β; MSP-α: Macrophage Stimulating Protein α Chain; NGF: Nerve Growth Factor; NT-3/4: Neurotrophin-3/4; OPG: *Osteoprotegerin;* OSM: Oncostatin; SCF: Stem Cell Factor; SDF: Stromal Cell-Derived Factor 1; sgp130: soluble IL-6 receptor; sTNF RI/RII: soluble tumor necrosis factor receptor type I/II; TECK: Thymus Expressed Chemokine; TGF-β3: Transforming Growth Factor-β3; THPO: Thrombopoietin; TIMP-!/2: Tissue Inhibitor of Matrix Metalloproteinases-1/2; TNF-α/β: Tumor Necrosis Factor; TRAIL-R3/R4: TNF-related apoptosis-inducing ligand receptor-3/4; UPAR: Urokinase Plasminogen Activator Receptor; VEGF: Vascular Endothelial *Growth Factor*; *VEGF-D*: Vascular Endothelial *Growth Factor D*.

HB-EGF: Heparin-binding EGF-like Growth Factor; KGF: Keratinocyte Growth Factor; PDGF-BB: Platelet Derived Growth Factor.

BM: basal medium (no cells) CM: conditioned medium.

detected in hMSC cell lysates (Lys) and/or cell conditioned media (CMs) in respect to basal medium for culture (BM, in the absence of hMSCs) (Table 1A). In particular, factors knowingly involved in the regulation of the neurogenic niche, such as Epidermal Growth Factor (EGF), Brain Derived Growth Factor (BDNF) as well as Neurotrophin-3 (NT-3), were expressed and released by our cells *in vitro*. To further analyze the potential neuro-angiogenic support exerted by hMSC, we precisely quantified the consistent release of several molecules involved in NSC biology and homing towards lesioned areas, such as Vascular Endothelial Growth Factor (VEGF), Hepatocyte Growth Factor (HGF) and Fibroblast Growth Factor (FGF-2) by multiplex analysis in CMs from both proliferating (5 days in culture) and confluent (10 days in culture) hMSCs (Table 1B). The comparison between basal BM composition and CM (conditioned by cells) clearly identifies cytokines/growth factors specifically due to cellular production/release.

2.4. *Grafted hMSCs actively secreted BDNF in vivo*

Multiple neurogenic and neurorescue effects on several distal regions (SVZ and *SNpc*) likely require persistent release of growth factors able to promote cell migration/survival and neuronal differentiation. We therefore confirmed that grafted MSCs still retained the ability to synthesize BDNF, 23 days after implantation (Figs. 6F,G, BDNF+ cells, red), as confirmed by low (Fig. 6F) and high magnification (Fig. 6G) of labeled human cells. Interestingly, BDNF labeling is absent in lesioned PBS grafted animals (Fig. 6H). The long term expression of this neurotrophic factor sustains MSC contribution to the maintenance of the dopaminergic phenotype as well as SVZ neurogenesis. Conversely, GDNF was not detected in grafted hMSCs in any experimental conditions after 4 weeks (not shown).

3. Discussion

In this study, we used the well defined rat model of PD induced by unilateral intrastriatal injection of 6-OHDA (Deumens et al., 2002). The model is characterized by a slowly evolving and progressive nigrostriatal degeneration (Blandini et al., 2007; Sauer and Oertel, 1994), and resembles the progressive nature of the neurodegenerative process of human PD. In our experimental paradigm, hMSCs were transplanted, 5 days after the toxic insult, in an injured yet still actively degenerating environment, and significantly reduced the ongoing toxin-induced loss of dopaminergic terminals. The aims of our work were actually (1) to verify adult hMSC neuroglial potential *in vivo* and their capability to support DA neurons survival after 6-OHDA lesion in rats and (2) to test hMSC capability to boost neurogenesis in a pathological environment. Our data demonstrate that the reciprocal interactions between grafted hMSCs and 6-OHDA lesioned brains lead to neurorescue and neurogenic effects in two distal brain regions connected to the striatum by dopaminergic afferents in a rodent model of PD (as depicted in Fig. 7). Indeed, intrastriatal hMSC transplantation regionally protected dopaminergic terminals/soma in striatum/*SNpc*, as well as sustained proliferation and neuralization

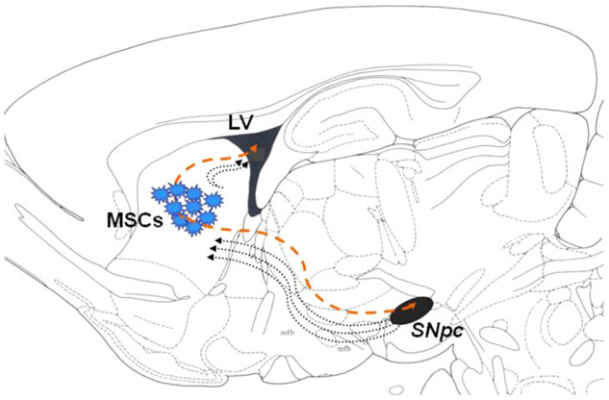

Fig. 7 – Diagram showing the multiple distal effects exerted by hMSC transplantation in the PD animal model. The reciprocal interactions between the lesioned brain and the grafted cells are not limited to site of implantation. hMSCs influence both SVZ neurogenesis and dopaminergic neurons survival in *SNpc* even in the absence of relevant specific dopaminergic neurogenesis. The distal influence of grafted cells may be related to the surviving dopaminergic afferents connecting the striatum to SVZ and *SNpc* (dotted lines). LV = Lateral Ventricle; *SNpc* = *Substantia Nigra pars compacta*; MFB = Medial Forebrain Bundle; MSCs = Mesenchymal Stem Cells.

of newborn cells inside SVZ, without affecting glial cell number. Our results indicate that transplantation of hMSCs in an accessible brain area can effectively enhance neuronal survival and sustain the specific development of immature cells towards neurons in an animal model of PD.

3.1. *Dopaminergic innervation and SVZ neurogenesis*

Studies in PD animal models have established that toxin-induced dopaminergic depletion alters neurogenesis, affecting the neural precursor pool biology (Geraerts et al., 2007; Hoglinger et al., 2004) and, directly and dose-dependently, impairs SVZ proliferation (Baker et al., 2004; He et al., 2006, 2008). In addition, preservation of an intact dopaminergic nigro-ventricular innervation is crucial to sustain neurogenesis (Baker et al., 2004), especially in aged subjects (Freundlieb et al., 2006). Consequently, therapeutic strategies based on the modulation of endogenous neuroregeneration have been proposed as an alternative to direct substitution of damaged/lost DA neurons (Geraerts et al., 2007).

Through the combined detection of two cell cycle markers (Ki67 and PCNA), and antigens of neural progenitors (Nestin) or migrating neuroblasts (Dcx), we evaluated the distal effects of hMSC transplantation on the host neurogenic activity. For the first time, our results demonstrated that transplantation of adult hMSCs in 6-OHDA lesioned animals propelled local microenvironmental signals and sustained the physiological SVZ cell proliferation in the long term. A similar increased neurogenesis has been previously observed following intrastriatal transplantation of embryonic NSCs in parkinsonian rats (Yasuhara et al., 2006). We also show that the hMSCs-dependent increased neurogenesis is accompanied by

transformation of progenitor cells into neuroblasts (Type A) actively migrating towards the lesioned striatum, as described in physiological neurogenesis (Doetsch et al., 1999). Interestingly, our data demonstrated that boosted persisting proliferation and neuronal maturation in the SVZ were clearly dependent on the amount of transplanted hMSCs and required the presence of lesioned striata; indeed, no enhancement of neurogenesis was observed following transplantation in SHAM animals, irrespectively to grafted cell dose. Enhancement of proliferation and neuralization in SVZ maintained comparable astrocyte number in all experimental conditions, with a slight increase of glial hypertrophy, both in lesioned and contralateral hemisphere in presence of high dose cell graft.

The long term beneficial neurogenic effects we observed following hMSC transplantation might, in part, correlate with the intact nigro-subventricular innervation, crucial for the regulation of SVZ proliferation and neurogenesis (Baker et al., 2004), still present at the time of transplantation (Blandini et al., 2007). 6-OHDA-induced lesion has been shown to impair SVZ proliferation (Baker et al., 2004), directly and dose-dependently. The neutoxin-induced DA depletion seems to bring on an immediate proliferation of neural precursors, both in rodents (Aponso et al., 2008; Liu et al., 2006; Winner et al., 2006) and primates (Freundlieb et al., 2006), that returns to physiological levels with time (Aponso et al., 2008; Liu et al., 2006). The observed activation phenomena, especially neuronal maturation, may, however, be adequately supported in the long term through the continuous infusion of growth factors (de Chevigny et al., 2008) or following transplantation of cells secreting trophic factors (Arias-Carrion et al., 2006; Belzunegui et al., 2008). Analogously, SVZ cells are highly vulnerable to the acute or subacute administration of 1-methyl-4-phenyl-1,2,3,6-tetrahydropyridine (MPTP), in mice (He et al., 2006, 2008). Interestingly, MPTP neurotoxicity appears to affect migrating Dcx+ neuroblasts, reducing their number in SVZ and rostral migratory stream by means of apoptotic cell death activation (He et al., 2008). Conversely, in the same animal model, increased neurogenesis is obtained by long term infusion of FGF-2 (Peng et al., 2008), thus demonstrating that neuroblast cell death may be recovered.

Aponso et al. have recently reported increased progenitor cell proliferation and astrogenesis in the same model used in our study (partial progressive 6-OHDA induced lesion), in the absence of newly generated neuronal progenitors (Aponso et al., 2008). Our paper reports comparable results in terms of activation of SVZ proliferation after 6-OHDA lesion with minimal experimental differences. Interestingly, in the absence of cell transplantation, Aponso does not observe augmented Dcx expression and describes striatal induction of astrogenesis. Conversely, our results suggest that reciprocal influences between grafted cells and endogenous neural precursors support continuative proliferation and selective shift towards specific neuralization of SVZ progenitor cells, within the lesioned striata, without affecting the glial cell number. Comparable results have been previously presented in an acute PD model (6-OHDA injection in the Medial Forebrain Bundle, (Winner et al., 2009)). Moreover, the selective proliferation of SVZ neuroblasts, but not astrocytes, deserves to be further investigated since the newborn neurons could possibly originate dopaminergic neurons by phenotypic shift, as previously demonstrated (Tande et al., 2006).

3.2. *Neuroprotective/neurorescue effects of hMSCs and cytokine release*

This positive effect did not require the acquisition of neuronal phenotype by hMSCs *in situ* and may rely on an effective support to injured neurons through the local release of soluble factors in striatum (Bai et al., 2007a; Caplan and Dennis, 2006; Isele et al., 2007).

Our qualitative analysis demonstrated that naïve hMSCs consistently synthesize a variety of trophic factors, besides the known canonical hematopoietic groups related to the active role of hMSCs in bone marrow microenvironment (Han et al., 2006). The positive immunomodulatory effects exerted by hMSCs via soluble factors (Krampera et al., 2006) and potentially released by the transplanted human cells *in situ* might be determinant in directly counteracting the PD-associated inflammatory processes known to influence oxidative injuries (Litvan et al., 2007) and apoptotic pathways (Hodaie et al., 2007). Accordingly, the continuous infusion of erythropoietin, a hematopoietic hormone, has neuroprotective effects against 6-OHDA toxicity *in vivo* (Kadota et al., 2009), with preservation of striatal TH-positive fibers comparable to our data. Neuroprotection also correlated with a dose-dependent phenotypic change of the human cells in response to the local (degenerated) surrounding: implantation of Low hMSCs amounts generated Nestin-containing grafts, while considerable astroglial marker acquisition, completely absent in cultures, was detected only when higher cell amounts were used. No TH- and DAT-positive hMSCs were detected *in vivo*, indicating that, unlike embryonic stem cells (Bjorklund et al., 2002), our cells did not acquire a dopaminergic phenotype after transplantation. Similarly, no TH-positive donor cells were found within grafted fetal-derived NSC line (Yasuhara et al., 2006) and only limited dopaminergic fate acquisition has been previously shown for naïve (Li et al., 2001) or transfected stromal cells (Kim et al., 2006). It is noteworthy that grafted cells in SHAM animals readily survived without detectable effects on TH neurons density, in the absence of immunopositivity for neural antigens, regardless of the cell dose. Therefore, crosstalk between implant and the lesioned surroundings appears to influence the positive outcome of transplantation in a dose-dependent manner.

Taken together, our results demonstrate the existence of an intricate interaction between the grafted hMSCs and the lesioned local surrounding. Only the presence of an ongoing degenerative process within the DA-depleted striatum enhanced neural differentiation of transplanted cells, which in turn, reduced the toxin-induced dopaminergic neurodegeneration. A clear shift towards a neuronal phenotype was not necessary for the beneficial effects to manifest (Gonzalo-Gobernado et al., 2009). The observed dopaminergic neuronal sparing, coupled to SVZ neurogenesis, proves that, in principle, dampening the pathological cell loss may not merely depend upon orthotopic dopaminergic neurogenesis (Hermann and Storch, 2008), but may exploit alternative neurorescue mechanisms, as previously demonstrated for

intracerebroventricular growth factor infusion (Gonzalo-Gobernado et al., 2009).

Previous studies have shown that developmental and/or remodeling mechanisms depend on the release of growth factors capable of specifically influencing distal regions and efficiently promoting endogenous CNS repair (Okano et al., 2007; Ormerod et al., 2008; Shen et al., 2004). It has also been suggested that mesenchyme-derived cells may influence brain plasticity by means of circulating factors critical for neural stem cell (NSC)-niche and crucial for CNS repair (Okano et al., 2007; Shen et al., 2004). In the brain, NSCs are known to reside in highly vascularized niches where complex, dynamic interplays between neurons and endothelial cells are mediated via neurotrophines/cytokines (Okano et al., 2007). Some of the hMSC-dependent factors we detected *in vitro*, including VEGF and several components of the FGF family, are known to play defined roles in neural development, remodeling and neurorescuing within the basal ganglia after brain injury (Okano et al., 2007; Yasuhara et al., 2005). Importantly, we show that grafted hMSCs still express BDNF 4 weeks after transplantation indicating their capability to maintain their phenotype even under non-physiological conditions. Interestingly, BDNF is a neurotrophic factor involved in regulating survival and differentiation of neurons during development (Schwartz et al., 1997) and may be responsible for the striatal/nigral dopaminergic survival we observed. Although we could not report GDNF expression in hMSCs *in vivo*, this neurotrophic factor may be not detectably expressed at the end point we chose (4 weeks), therefore additional analysis may clarify this specific topic.

Moreover, hMSCs also expressed inflammatory mediators (as CCL5/Rantes, CCL2/MCP1) and growth factors involved in the NSC bystander effect, recently proposed as an additional reparative mechanism (Martino and Pluchino, 2006). Long-term benefits of cell therapy may therefore rely on the reconstitution of the endogenous NSC compartment, via an atypical enriched ectopic (perivascular) niche (Martino and Pluchino, 2006), an environment closely resembling our transplanted setting. Previous studies have indicated that MSCs may influence NSC differentiation *in vitro* (Bai et al., 2007a,b; Rivera et al., 2006). Our results suggest that close interactions between the lesioned striatal environment and hMSCs *in vivo* are required to observe enhanced neurogenesis in SVZ *in vivo*. Indeed, no signs of regeneration were observed either in lesioned animals in the absence of transplanted human cells or in SHAM animals that received hMSCs. In view of future clinical applications, we decided to perform all the experiments in the presence of daily treatment with cyclosporine. The immunosuppressive treatment *per se* had no effect on the distribution and survival of transplanted hMSCs, the progression of the 6-OHDA-induced neuronal cell loss, or the typical glial response that parallel both neurodegenerative and grafting processes. Therefore, the beneficial outcome we observed must be directly correlated to the presence of hMSCs and not to possible side effects of cyclosporine treatment.

Our results demonstrate that SCs may act locally on neuronal replacement and may thus stimulate the brain to repair, at least partially, established pathological damages. Furthermore, our data suggest that specific substances/cytokines are involved in the mechanism of neuronal rescue, a topic which is actually under further investigation.

4. Conclusion

In conclusion, our data show that striatal grafting of hMSCs can (1) preserve dopaminergic neurons and (2) enhance neurogenesis in a rodent model of PD, based on the intrastriatal infusion of 6-OHDA. Our results suggest alternative ways to slow down neuronal cell loss and possibly regenerate affected brain areas. The direct influence of hMSCs towards damaged cerebral tissues may provide novel insights for the development of therapeutic strategies, aiming to contrast the neurodegenerative processes of PD. The discovery of the specific molecules involved in these biological events could also shed light on new pharmacological disease-modifying treatments and novel potential targets, readily applicable to patients.

5. Experimental procedures

5.1. *Preparation and analysis of hMSC samples*

Commercial hMSCs (Cambrex, Walkersville, MD, USA) as well as the specific medium (MSCBM, Cambrex) were purchased and adherent cells were grown, until confluence, following the manufacturer's instructions. Several different commercial batches ($n=6$) were utilized to exclude generic unspecific effects related to a single cell culture. Vitality maintenance was tested on cell cultures and hMSC transplanted tissues by TUNEL analysis using the In Situ Cell Death Detection Kit, TMR-red (Roche, Hoffmann–La Roche Ltd, Basel, Switzerland). To exclude possible chromosome aberrations, cultures were expanded *in vitro* for no more than three passages and subjected to karyotypic analysis (using Quinacrine coloration standard karyotipic analysis and fluorescent *in situ hybridization*), as previously described (Mitalipova et al., 2005). All treatment conditions were replicated twice using at least three independent cell cultures.

The day before implantation, cells were loaded overnight with the fluorescent vital dye Hoechst 33258 (1 ng/ml; Molecular Probes-Invitrogen) in order to directly visualize transplanted cells in tissue sections without further procedures (Zhang and Kiechle, 2001).

5.2. *In vivo procedures*

All animal care and use were in accordance with the European Convention for Animal Care and Use of Laboratory Animals, and were approved by the Veterinarian Department of the Italian Ministry of Health. Male Sprague–Dawley rats (Charles River, Calco, LC, Italy), weighing 200 g at the beginning of the experiment, were housed two per cages at 20–22 °C on a 12 h light/dark cycle, with food and water available ad libitum.

All surgical procedures were conducted under aseptic conditions. Animals were anaesthetized with 50 mg/kg of

sodium-thiopental (50 mg/kg; Hospira, Lake Forest, IL) and arbitrarily divided into two groups. Rats were then placed in a stereotaxic frame (Stoelting, Wood Dale, IL, USA) and 3 μl containing 20 μg of 6-OHDA (Sigma-Aldrich) in saline/0.02% ascorbate (Sigma-Aldrich; 6-OHDA group, $n=26$), or vehicle (saline/ascorbate) alone (SHAM group, $n=18$), were injected into the right striatum (1.0 mm anterior, 3.0 mm lateral and 5.0 mm ventral, with respect to bregma and dura (Paxinos and Watson, 1998) as described before (Blandini et al., 2007)). Five days later, animals in each group were further divided into three subgroups ($n=6$–10/group) and transplanted (8 μl/rat) along two tracts per striatum (1.8 mm anterior, 3.0 mm lateral and 5.0 mm ventral, and 0.2 mm anterior, 3.0 mm lateral and 5.0 mm ventral with respect to bregma and dura) as follows: (1) PBS (6-OHDA-PBS and SHAM-PBS group), (2) 32,000 hMSCs (6-OHDA-Low and SHAM-Low group), and (3) 180,000 hMSCs (6-OHDA-high and SHAM-high group). To avoid possible reject of the xenotransplant and to mimic standard clinical procedures, all animals received a daily injection of cyclosporine A, a treatment that *per se* had no influence on either the 6-OHDA-induced neurodegenerative process or transplanted human cells. In order to exclude possible complicating effects of cyclosporine, we performed preliminary experiments even in the absence of cyclosporine, clearly indicating no differences between the two conditions (see Supplemental Fig. 1).

All intracerebral infusions were performed at 0.5 μl/min, using a Hamilton 10-μl syringe with a 26-gauge needle and, to avoid reflux along inoculation track, the needle was left in place for 10 min before being retracted.

5.3. *Immunocytochemical studies on cell cultures (ICC) and immunohistochemical analysis on frozen sections (IHC)*

Cultured hMSCs were permeabilized and incubated at 37 °C for 1 h with the appropriate primary antibodies in 10% Normal Goat Serum (NGS) and 0.3% Triton X-100 (all Sigma-Aldrich, St. Louis, MO, USA) after a fixation step with 4% paraformaldehyde (PFA) in 0.1 M PBS (pH 7.4) for 20 min (Ratti et al., 2006). Secondary antibodies were utilized as specified below in the tissue staining section.

For IHC preparations, animals were sacrificed 28 days post lesion by transcardiac perfusion, under deep anesthesia, with ice-cold PBS followed by 4% PFA (0.1 M PBS). Briefly, post-fixed, cryopreserved brain were cut in serial coronal sections (20 μm thick), containing the striatum, using a cryostat (Leica CM 1850 UV; Leica Microsystems Ltd, Heidelberg, Germany). Brain slices were incubated overnight at 4 °C with the specific antibodies, diluted in 0.1 M PBS containing 0.1% Triton X-100 and 3% NGS. Tyrosine hydroxylase-immunohistochemistry (TH) was performed on brain tissues as previously described (Blandini et al., 2007) using the specific Chemicon antibody diluted 1:1000. Additionally markers for rodent proliferating neural progenitors were respectively Ki67 (1:500; Novacastra, Carlsbad, CA, USA), PCNA (IHC 1:200; DAKO, Glostrup, Denmark), double cortin (Dcx, IHC 1:100; Cell Signaling, Beverly, MA, USA), S100b (IHC 1:200; Abcam, Cambridge, UK) and GFAP (IHC 1:500; Chemicon). Cultured and transplanted cells were also characterized for the expression of human specific GFAP (ICC 1:100; IHC 1:500), and Nestin (ICC 1:100; IHC 1:300) both from Chemicon (Chemicon International Inc., Temecula, CA, USA). Furthermore, the human origin of grafts was confirmed using the specific human Nuclear Mitotic Apparatus Protein 1 (NuMA) nuclear antigen (ICC 1:100; IHC 1:50; Chemicon) in order to unambiguously identify them, thus excluding Hoechst diffusion to host cells (Iwashita et al., 2000). Human specific antigens were utilized to confirm the specific origin of grafted hMSCs only in the striatum where cells were implanted. TUNEL analysis was also performed on both cultured/grafted hMSCs to check apoptotic events both *in vitro* and *in vivo*, while proliferative hMSCs were detected as Ki67/Hoechst double+ cells. The detection of neurotrophines BDNF (IHC 1:50, Abcam) and GDNF (IHC 1:50, Abcam) were further assayed.

All the used antibodies were preliminary tested on the related cell cultures/tissues and negative controls to assure their specificity. Secondary fluorescent antibodies (all from Jackson ImmunoResearch, Chicago, IL, USA), in 0.1 M PBS containing 0.1% Triton X-100 and 3% NGS, were utilized: Cy2 monoclonal goat anti-mouse (ICC 1:200); Cy3 polyclonal goat anti-rabbit (ICC 1:500); Cy2 polyclonal goat anti-rabbit (IHC 1:70); Cy3 monoclonal goat anti-mouse (IHC 1:500). All double labeling were conducted in combination with a nuclear counterstaining 4′,6-diamidino-2-phenylindole (DAPI, 0.3 μg/ml, Sigma-Aldrich). Finally samples were washed with PBS and mounted with Fluorsave® (Calbiochem, La Jolla, CA, USA) (Ratti et al., 2006). All fluorescent samples were viewed under a LeicaDMIRE2 microscope and image analysis was performed by blinded observers. Images were captured with a CCD camera directly connected to the analytical system (Leica Microsystems Ltd.).

5.4. *Morphological analysis*

Image analysis of TH immunohistochemistry and grafted Hoechst-positive hMSCs was performed using an AxioSkop 2 microscope connected to a computerized image analysis system (AxioCam MR5) equipped with a dedicated software (AxioVision Rel 4.2; Zeiss, Oberkochen, Germany).

For each animal, the optical densities of the TH-immunoreactive fibers in the striatum were measured at three rostrocaudal levels (AP 2.0, 0.8, and -0.4 mm with respect to bregma), considering three sections per level. Briefly, a picture of each section was captured at 1.25× magnification maintaining the same light and contrast intensities across all images. In both the intact and lesioned hemisphere, a region of interest was manually selected to include the entire striatal area and density analysis performed. Optical readings were corrected for non-specific background density, as measured from an area deprived of specific TH-staining. The mean optical value for each section was calculated and summed up for a given level. Results (mean ±SEM) are presented as the ratio of the value in the lesioned striatum with respect to the intact side.

A relative evaluation of surviving Hoechs+ hMSCs was performed on every sixth of 20-μm coronal sections throughout the entire transplanted striatum (modified from Yasuhara et al., 2006). The intersectional distance considered (120 μm) avoided possible bias of counting twice the same nuclei.

Briefly, for each section five visual fields randomly covering the striatal area were captured and Hoechst+ cells counted. Results were summed and an amount of Hoechst+ hMSCs attributed to each animal. A relative number of "surviving hMSCs" was thus calculated for each single treatment groups. The ratio of the mean values obtained from the group of animals that had received high and low amount of human cells was calculated (High/Low) and compared to the ratio at the time of transplantation (Supplemental Fig. 2C).

Neurogenesis rate was evaluated by quantification of PCNA and Ki67 fluorescent immunoreactivity in the SVZ lining the lateral ventricle. The original idea was to conduct a comprehensive study using PCNA in combination with Ki67 in order to discriminate, at least, proliferating vs. quiescent SVZ cells, thus avoiding BrdU limitations (Taupin, 2007).

To circumvent inaccurate assessment of unevenly distributed and aggregated proliferative cells, the whole SVZ area containing PCNA+ and/or Ki67+ cells was determined by digital image analysis (Aponso et al., 2008). Since in densely packed layers of cells is difficult to discriminate individual cell profiles other counting techniques (i.e. fractal analysis or stereological counting) cannot be used reliably, as recently demonstrated for CNS macrophages (Donnelly et al., 2009). Single cell counting on a restricted, although representative area at high magnification, was avoided and therefore, we evaluated the total immunoreactivity on every fifth serial section (100 μm apart) encompassing the entire SVZ area within the striatum (total section number=18) for each animal (n=4) in the specified experimental conditions (6-OHDA lesioned brains grafted with PBS/Low/High cell dose). Briefly, SVZ images (20×) from both the left (intact) and right (lesioned/transplanted) hemisphere were acquired using a fluorescent microscope (LeicaDMIRE2) maintaining fixed acquisition conditions. The whole area was reconstructed and optical density of PCNA and Ki67+ areas measured using the ImageJ 1.40s (National Institute of Health) software. The process of measuring the area occupied by labeled cells within a specific wide region appears optimal when individual cell are dispersed and their profiles cannot be clearly distinguished (Donnelly et al., 2009). A similar approach was utilized for Nestin quantification in the SVZ. Results (mean±SEM) are indicated as intensity signal and are expressed in function of both intensity and total area of PCNA/Ki67 or Nestin immunoreactivity in the ipsilateral SVZ compared to the contralateral (CLT) one.

5.5. *Human cytokine array protocol*

One hundred twenty different active cytokines/chemokines and neurotrophic proteins were profiled with Human Antibody Array kit (divided on two different membranes; RayBiotech Inc, Norcross, GA, USA) in both 7 days conditioned media (CMs) (500 μl, Array C-1000) and cell lysates (300 μg, Array C-1000.1). Conditioned media (CMs), obtained from proliferating MSCs in culture, were centrifuged at 1000 × g for 15 min and chilled rapidly in liquid nitrogen. Samples were treated as stated in the directions from the manufacturer and relative signals detected on Hyperfilms (Amersham Bioscience, Chicago, IL, USA). Cytokine autoradiograms were scanned and semi-quantitative densitometric analysis performed, in triplicates, using a dedicated software (Quantity One-BioRad, Richmond, CA, USA). Detected signal intensity was directly related to cytokine levels and was evaluated on constant area, afterward subtraction of autoradiogram background. CM levels were always compared to BM ones (in the absence of MSC) in order to exclude inaccurate growth factor detection. Values were expressed as increased/decreased expression in CM compared to BM levels (respectively metabolic secretion/uptake as specified in Table 1A) and as present (+) or absent (-) in LYS.

5.6. *Multiplex analysis*

Similarly, CMs, obtained from proliferating or MSC cultures at confluence (respectively around 5 or 10 days in culture) were centrifuged at 1000 × g for 15 min and chilled rapidly in liquid nitrogen. Cytokine determination for the quantification of several neurovascular agents in BM and CM (both 1:2 or undiluted) was performed by Searchlight Multiplex Angiogenesis ELISA Analysis (Pierce Endogen, Rockford, IL, USA) following the manufacturer's instructions. All samples were plated in triplicate. Before the Streptavidin-*Horseradish Peroxidase* reagent addition, plates were sent to the commercial retailer, which performed the revelation, image acquisition as well as the calculation of results. The luminescence signal for every well was obtained directly, using the SEARCHLIGHT® CDCD Imaging and ANALYSIS SYSTEM also from Pierce Biotechnology, Inc. Image analysis and conversion of the raw data to pg/ml values required ARRAYVISION™ software (Imaging Research, Inc.).

5.7. *Statistical analysis*

All values are expressed as mean±SEM. Comparisons between groups were made using Student's t-test (paired) or one-way analysis of variance (ANOVA, nonparametric) followed by a Tukey's HSD or Dunnet *post hoc* test, as specified in the respective figure legends, using a dedicated statistical software (Prism 3 software, GraphPad Software, San Diego, CA, USA). The minimum level of statistical significance was set at $p<0.05$.

6. Competing interests statement

The authors declare that they have no competing financial interests.

7. Author contribution

FB and VS supervised the overall project and the manuscript drafting
EP and GN critically contributed to project conception and manuscript edition
EZ, LC, MTA performed the immunocytochemical/histological data
CC, LC, MM executed molecular analysis on hMSC neurotrophines release
PB expanded hMSCs and confirmed their stromal origin

MTA conducted the transplantation experiments with GB kind help
MTA and LC wrote the paper

Acknowledgments

We dedicate this work to the loving memory of Prof. Davide Soligo (†). We wish to thank Dr. D. Giardino and the Laboratory of Medical Cytogenetics and Molecular Genetics, IRCCS Istituto Auxologico Italiano, Milan, Italy for the karyotipic analysis and the helpful technical support.

This work was supported by Italian Ministry of Health, (ex art.56 2004), Fondazione Cariplo, AIL (Associazione Italiana Leucemie) and by a Francesco Caleffi donation.

Appendix A. Supplementary data

Supplementary Figure 1. Immuno-suppression with cyclosporine resulted ineffective on both hMSCs distribution and number. Representative fields of contralateral (A,B) vs. lesioned striata implanted with hMSCs (C,D) demonstrated that experimental procedures, but not cyclosporine treatments, influence localized astroglial and microglial responses without affecting hMSC integration/proliferation. S100b+ cells (red) and GFAP+ cells (green); scale bar: 50 μm.

Supplemental Fig. 2. Grafted cells are dose dependent present in implanted striatum 23 days after lesion. Low magnification of 32.0000 (A) and 180.000 (B) Hoechst positive hMSCs 23 days after transplantation (T28, days from lesion): transplanted cells are dose-dependently dispersed around injection track; scale bar: 200 μm. (C) Relative evaluation of High/Low hMSC ratio in 6-OHDA-lesioned animals. Pre indicates the actual ratio (5.7) at the time of transplantation; post indicates the ratio of the number of Hoechst-positive cells observed *in situ*, 23 days after transplantation in the 6-OHDA-High and 6-OHDA-Low groups. (D) Percentage of TH-positive fibers at three different striatal coronal levels (from bregma) in grafted 6-OHDA-lesioned animals ($n=6/10$). Graphic legend: ■=6-OHDA-PBS, ▩=6-OHDA-Low, □=6-OHDA-High. Results (mean±SEM) are expressed as the density (%) of TH-positive fibers in the injected striatum respect to the intact hemisphere. $^{*}p<0.01$ vs. 6-OHDA-vehicle group (ANOVA followed by post hoc Dunnett's test).

Note: The supplementary material accompanying this article is available at (doi:10.1016/j.brainres.2009.11.041).

REFERENCES

Aponso, P.M., Faull, R.L., Connor, B., 2008. Increased progenitor cell proliferation and astrogenesis in the partial progressive 6-hydroxydopamine model of Parkinson's disease. Neuroscience 151 (4), 1142–1153.

Arias-Carrion, O., Hernandez-Lopez, S., Ibanez-Sandoval, O., Bargas, J., Hernandez-Cruz, A., Drucker-Colin, R., 2006. Neuronal precursors within the adult rat subventricular zone differentiate into dopaminergic neurons after substantia nigra lesion and chromaffin cell transplant. J. Neurosci. Res. 84 (7), 1425–1437.

Bai, L., Caplan, A., Lennon, D., Miller, R.H., 2007a. Human mesenchymal stem cells signals regulate neural stem cell fate. Neurochem. Res. 32 (2), 353–362.

Bai, L., Caplan, A., Lennon, D., Miller, R.H., 2007b. Human mesenchymal stem cells signals regulate neural stem cell fate. Neurochem. Res. 32 (2), 353–362.

Baker, S.A., Baker, K.A., Hagg, T., 2004. Dopaminergic nigrostriatal projections regulate neural precursor proliferation in the adult mouse subventricular zone. Eur. J. Neurosci. 20 (2), 575–579.

Belzunegui, S., Izal-Azcarate, A., San Sebastian, W., Garrido-Gil, P., Vazquez-Claverie, M., Lopez, B., Marcilla, I., Luquin, M.R., 2008. Striatal carotid body graft promotes differentiation of neural progenitor cells into neurons in the olfactory bulb of adult hemiparkisonian rats. Brain Res. 1217, 213–220.

Bjorklund, L.M., Sanchez-Pernaute, R., Chung, S., Andersson, T., Chen, I.Y., McNaught, K.S., Brownell, A.L., Jenkins, B.G., Wahlestedt, C., Kim, K.S., Isacson, O., 2002. Embryonic stem cells develop into functional dopaminergic neurons after transplantation in a Parkinson rat model. Proc. Natl. Acad. Sci. U. S. A. 99 (4), 2344–2349.

Blandini, F., Levandis, G., Bazzini, E., Nappi, G., Armentero, M.T., 2007. Time-course of nigrostriatal damage, basal ganglia metabolic changes and behavioural alterations following intrastriatal injection of 6-hydroxydopamine in the rat: new clues from an old model. Eur. J. Neurosci. 25 (2), 397–405.

Blandini, F., Armentero, M.T., Martignoni, E., 2008. The 6-hydroxydopamine model: news from the past. Parkinsonism Relat. Disord. 14 (Suppl. 2), S124–129.

Borta, A., Hoglinger, G.U., 2007. Dopamine and adult neurogenesis. J. Neurochem. 100 (3), 587–595.

Caplan, A.I., Dennis, J.E., 2006. Mesenchymal stem cells as trophic mediators. J. Cell. Biochem. 98 (5), 1076–1084.

Coronas, V., Bantubungi, K., Fombonne, J., Krantic, S., Schiffmann, S.N., Roger, M., 2004. Dopamine D3 receptor stimulation promotes the proliferation of cells derived from the post-natal subventricular zone. J. Neurochem. 91 (6), 1292–1301.

Dass, B., Olanow, C.W., Kordower, J.H., 2006. Gene transfer of trophic factors and stem cell grafting as treatments for Parkinson's disease. Neurology 66 (10 Suppl. 4), S89–103.

de Chevigny, A., Cooper, O., Vinuela, A., Reske-Nielsen, C., Lagace, D.C., Eisch, A.J., Isacson, O., 2008. Fate mapping and lineage analyses demonstrate the production of a large number of striatal neuroblasts after transforming growth factor alpha and noggin striatal infusions into the dopamine-depleted striatum. Stem Cells 26 (9), 2349–2360.

Deumens, R., Blokland, A., Prickaerts, J., 2002. Modeling Parkinson's disease in rats: an evaluation of 6-OHDA lesions of the nigrostriatal pathway. Exp. Neurol. 175 (2), 303–317.

Dezawa, M., Hoshino, M., Ide, C., 2005. Treatment of neurodegenerative diseases using adult bone marrow stromal cell-derived neurons. Expert Opin. Biol. Ther. 5 (4), 427–435.

Doetsch, F., Caille, I., Lim, D.A., Garcia-Verdugo, J.M., Alvarez-Buylla, A., 1999. Subventricular zone astrocytes are neural stem cells in the adult mammalian brain. Cell 97 (6), 703–716.

Donnelly, D.J., Gensel, J.C., Ankeny, D.P., van Rooijen, N., Popovich, P.G., 2009. An efficient and reproducible method for quantifying macrophages in different experimental models of central nervous system pathology. J. Neurosci. Methods 181 (1), 36–44.

Freundlieb, N., Francois, C., Tande, D., Oertel, W.H., Hirsch, E.C., Hoglinger, G.U., 2006. Dopaminergic substantia nigra neurons project topographically organized to the subventricular zone and stimulate precursor cell proliferation in aged primates. J. Neurosci. 26 (8), 2321–2325.

Geraerts, M., Krylyshkina, O., Debyser, Z., Baekelandt, V., 2007. Concise review: therapeutic strategies for Parkinson disease

based on the modulation of adult neurogenesis. Stem Cells 25 (2), 263–270.
Giordano, A., Galderisi, U., Marino, I.R., 2007. From the laboratory bench to the patient's bedside: an update on clinical trials with mesenchymal stem cells. J. Cell. Physiol. 211 (1), 27–35.
Gonzalo-Gobernado, R., Reimers, D., Herranz, A.S., Diaz-Gil, J.J., Osuna, C., Asensio, M.J., Baena, S., Rodriguez-Serrano, M., Bazan, E., 2009. Mobilization of neural stem cells and generation of new neurons in 6-OHDA-lesioned rats by intracerebroventricular infusion of liver growth factor. J. Histochem. Cytochem. 57 (5), 491–502.
Han, W., Yu, Y., Liu, X.Y., 2006. Local signals in stem cell-based bone marrow regeneration. Cell Res. 16 (2), 189–195.
He, X.J., Nakayama, H., Dong, M., Yamauchi, H., Ueno, M., Uetsuka, K., Doi, K., 2006. Evidence of apoptosis in the subventricular zone and rostral migratory stream in the MPTP mouse model of Parkinson disease. J. Neuropathol. Exp. Neurol. 65 (9), 873–882.
He, X.J., Yamauchi, H., Uetsuka, K., Nakayama, H., 2008. Neurotoxicity of MPTP to migrating neuroblasts: studies in acute and subacute mouse models of Parkinson's disease. Neurotoxicology 29 (3), 413–420.
Hermann, A., Storch, A., 2008. Endogenous regeneration in Parkinson's disease: do we need orthotopic dopaminergic neurogenesis? Stem Cells 26 (11), 2749–2752.
Hodaie, M., Neimat, J.S., Lozano, A.M., 2007. The dopaminergic nigrostriatal system and Parkinson's disease: molecular events in development, disease, and cell death, and new therapeutic strategies. Neurosurgery 60 (1), 17–28 discussion 28–30.
Hoglinger, G.U., Rizk, P., Muriel, M.P., Duyckaerts, C., Oertel, W.H., Caille, I., Hirsch, E.C., 2004. Dopamine depletion impairs precursor cell proliferation in Parkinson disease. Nat. Neurosci. 7 (7), 726–735.
Isele, N.B., Lee, H.S., Landshamer, S., Straube, A., Padovan, C.S., Plesnila, N., Culmsee, C., 2007. Bone marrow stromal cells mediate protection through stimulation of PI3-K/Akt and MAPK signaling in neurons. Neurochem. Int. 50 (1), 243–250.
Iwashita, Y., Crang, A.J., Blakemore, W.F., 2000. Redistribution of bisbenzimide Hoechst 33342 from transplanted cells to host cells. NeuroReport 11 (5), 1013–1016.
Kadota, T., Shingo, T., Yasuhara, T., Tajiri, N., Kondo, A., Morimoto, T., Yuan, W.J., Wang, F., Baba, T., Tokunaga, K., Miyoshi, Y., Date, I., 2009. Continuous intraventricular infusion of erythropoietin exerts neuroprotective/rescue effects upon Parkinson's disease model of rats with enhanced neurogenesis. Brain Res. 1254, 120–127.
Kim, S.U., Park, I.H., Kim, T.H., Kim, K.S., Choi, H.B., Hong, S.H., Bang, J.H., Lee, M.A., Joo, I.S., Lee, C.S., Kim, Y.S., 2006. Brain transplantation of human neural stem cells transduced with tyrosine hydroxylase and GTP cyclohydrolase 1 provides functional improvement in animal models of Parkinson disease. Neuropathology 26 (2), 129–140.
Krampera, M., Pasini, A., Pizzolo, G., Cosmi, L., Romagnani, S., Annunziato, F., 2006. Regenerative and immunomodulatory potential of mesenchymal stem cells. Curr. Opin. Pharmacol. 6 (4), 435–441.
Li, Y., Chen, J., Wang, L., Zhang, L., Lu, M., Chopp, M., 2001. Intracerebral transplantation of bone marrow stromal cells in a 1-methyl-4-phenyl-1,2,3,6-tetrahydropyridine mouse model of Parkinson's disease. Neurosci. Lett. 316 (2), 67–70.
Litvan, I., Chesselet, M.F., Gasser, T., Di Monte, D.A., Parker Jr., D., Hagg, T., Hardy, J., Jenner, P., Myers, R.H., Price, D., Hallett, M., Langston, W.J., Lang, A.E., Halliday, G., Rocca, W., Duyckaerts, C., Dickson, D.W., Ben-Shlomo, Y., Goetz, C.G., Melamed, E., 2007. The etiopathogenesis of Parkinson disease and suggestions for future research. Part II. J. Neuropathol. Exp. Neurol. 66 (5), 329–336.
Liu, B.F., Gao, E.J., Zeng, X.Z., Ji, M., Cai, Q., Lu, Q., Yang, H., Xu, Q.Y., 2006. Proliferation of neural precursors in the subventricular zone after chemical lesions of the nigrostriatal pathway in rat brain. Brain Res. 1106 (1), 30–39.
Martino, G., Pluchino, S., 2006. The therapeutic potential of neural stem cells. Nat. Rev., Neurosci. 7 (5), 395–406.
Mitalipova, M.M., Rao, R.R., Hoyer, D.M., Johnson, J.A., Meisner, L.F., Jones, K.L., Dalton, S., Stice, S.L., 2005. Preserving the genetic integrity of human embryonic stem cells. Nat. Biotechnol. 23 (1), 19–20.
Nam, S.C., Kim, Y., Dryanovski, D., Walker, A., Goings, G., Woolfrey, K., Kang, S.S., Chu, C., Chenn, A., Erdelyi, F., Szabo, G., Hockberger, P., Szele, F.G., 2007. Dynamic features of postnatal subventricular zone cell motility: a two-photon time-lapse study. J. Comp. Neurol. 505 (2), 190–208.
Okano, H., Sakaguchi, M., Ohki, K., Suzuki, N., Sawamoto, K., 2007. Regeneration of the central nervous system using endogenous repair mechanisms. J. Neurochem. 102 (5), 1459–1465.
Ormerod, B.K., Palmer, T.D., Caldwell, M.A., 2008. Neurodegeneration and cell replacement. Philos. Trans. R. Soc. Lond., B Biol. Sci. 363 (1489), 153–170.
Paxinos, G., Watson, C., 1998. The Rat Brain in Stereotaxic Coordinates, 4th ed. Academic Press, San Diego, USA.
Peng, J., Xie, L., Jin, K., Greenberg, D.A., Andersen, J.K., 2008. Fibroblast growth factor 2 enhances striatal and nigral neurogenesis in the acute 1-methyl-4-phenyl-1,2,3,6-tetrahydropyridine model of Parkinson's disease. Neuroscience 153 (3), 664–670.
Quinones-Hinojosa, A., Sanai, N., Soriano-Navarro, M., Gonzalez-Perez, O., Mirzadeh, Z., Gil-Perotin, S., Romero-Rodriguez, R., Berger, M.S., Garcia-Verdugo, J.M., Alvarez-Buylla, A., 2006. Cellular composition and cytoarchitecture of the adult human subventricular zone: a niche of neural stem cells. J. Comp. Neurol. 494 (3), 415–434.
Rasmusson, I., 2006. Immune modulation by mesenchymal stem cells. Exp. Cell Res. 312 (12), 2169–2179.
Ratti, A., Fallini, C., Cova, L., Fantozzi, R., Calzarossa, C., Zennaro, E., Pascale, A., Quattrone, A., Silani, V., 2006. A role for the ELAV RNA-binding proteins in neural stem cells: stabilization of Msi1 mRNA. J. Cell. Sci. 119 (Pt 7), 1442–1452.
Rivera, F.J., Couillard-Despres, S., Pedre, X., Ploetz, S., Caioni, M., Lois, C., Bogdahn, U., Aigner, L., 2006. Mesenchymal stem cells instruct oligodendrogenic fate decision on adult neural stem cells. Stem Cells 24 (10), 2209–2219.
Sauer, H., Oertel, W.H., 1994. Progressive degeneration of nigrostriatal dopamine neurons following intrastriatal terminal lesions with 6-hydroxydopamine: a combined retrograde tracing and immunocytochemical study in the rat. Neuroscience 59 (2), 401–415.
Schwartz, P.M., Borghesani, P.R., Levy, R.L., Pomeroy, S.L., Segal, R.A., 1997. Abnormal cerebellar development and foliation in BDNF-/- mice reveals a role for neurotrophins in CNS patterning. Neuron 19 (2), 269–281.
Shen, Q., Goderie, S.K., Jin, L., Karanth, N., Sun, Y., Abramova, N., Vincent, P., Pumiglia, K., Temple, S., 2004. Endothelial cells stimulate self-renewal and expand neurogenesis of neural stem cells. Science 304 (5675), 1338–1340.
Sundholm-Peters, N.L., Yang, H.K., Goings, G.E., Walker, A.S., Szele, F.G., 2005. Subventricular zone neuroblasts emigrate toward cortical lesions. J. Neuropathol. Exp. Neurol. 64 (12), 1089–1100.
Tande, D., Hoglinger, G., Debeir, T., Freundlieb, N., Hirsch, E.C., Francois, C., 2006. New striatal dopamine neurons in MPTP-treated macaques result from a phenotypic shift and not neurogenesis. Brain 129 (Pt. 5), 1194–1200.
Taupin, P., 2007. BrdU immunohistochemistry for studying adult neurogenesis: paradigms, pitfalls, limitations, and validation. Brain Res. Rev. 53 (1), 198–214.
Van Kampen, J.M., Eckman, C.B., 2006. Dopamine D3 receptor agonist delivery to a model of Parkinson's disease restores the nigrostriatal pathway and improves locomotor behavior. J. Neurosci. 26 (27), 7272–7280.

Van Kampen, J.M., Hagg, T., Robertson, H.A., 2004. Induction of neurogenesis in the adult rat subventricular zone and neostriatum following dopamine D3 receptor stimulation. Eur. J. Neurosci. 19 (9), 2377–2387.

Winner, B., Geyer, M., Couillard-Despres, S., Aigner, R., Bogdahn, U., Aigner, L., Kuhn, G., Winkler, J., 2006. Striatal deafferentation increases dopaminergic neurogenesis in the adult olfactory bulb. Exp. Neurol. 197 (1), 113–121.

Winner, B., Desplats, P., Hagl, C., Klucken, J., Aigner, R., Ploetz, S., Laemke, J., Karl, A., Aigner, L., Masliah, E., Buerger, E., Winkler, J., 2009. Dopamine receptor activation promotes adult neurogenesis in an acute Parkinson model. Exp. Neurol. 219 (2), 543–552.

Yasuhara, T., Shingo, T., Muraoka, K., Kameda, M., Agari, T., Wen Ji, Y., Hayase, H., Hamada, H., Borlongan, C.V., Date, I., 2005. Neurorescue effects of VEGF on a rat model of Parkinson's disease. Brain Res. 1053 (1–2), 10–18.

Yasuhara, T., Matsukawa, N., Hara, K., Yu, G., Xu, L., Maki, M., Kim, S.U., Borlongan, C.V., 2006. Transplantation of human neural stem cells exerts neuroprotection in a rat model of Parkinson's disease. J. Neurosci. 26 (48), 12497–12511.

Zhang, X., Kiechle, F., 2001. Hoechst 33342-induced apoptosis is associated with decreased immunoreactive topoisomerase I and topoisomerase I-DNA complex formation. Ann. Clin. Lab. Sci. 31 (2), 187–198.